Published in final edited form as:
Curr Biol. 2014 October 6; 24(19): 2247–2256. doi:10.1016/j.cub.2014.08.021.

A temporal channel for information in sparse sensory coding

Nitin Gupta[*] and **Mark Stopfer**
National Institute of Child Health and Human Development, National Institutes of Health, Bethesda, MD 20892, USA

Summary

Background—Sparse codes are found in nearly every sensory system, but the role of spike timing in sparse sensory coding is unclear. Here we used the olfactory system of awake locusts to test whether the timing of spikes in Kenyon cells, a population of neurons that responds sparsely to odors, carries sensory information to, and influences the responses of, follower neurons.

Results—We characterized two major classes of direct followers of Kenyon cells. With paired intracellular and field potential recordings made during odor presentations, we found these followers contain information about odor identity in the temporal patterns of their spikes, rather than in the spike rate, the spike phase or the identities of the responsive neurons. Subtly manipulating the relative timing of Kenyon cell spikes with temporally and spatially structured microstimulation reliably altered the response patterns of the followers.

Conclusions—Our results show that even remarkably sparse spiking responses can provide information through stimulus-specific variations in timing on the order of tens to hundreds of milliseconds, and that these variations can determine the responses of downstream neurons. These results establish the importance of spike timing in a sparse sensory code.

Introduction

Brain circuits encode sensory information into a variety of neural representations. These representations range from dense, time-varying patterns of intense spiking in overlapping sets of neurons to sparse spikes in just a few selective neurons. Sparse codes are used by nearly all sensory systems[1] including vision[2] (but see [3]), audition[4], somatosensation[5], and olfaction[6]. In dense spiking codes, the precise timing of spikes has been shown to contain sensory information[7], but, despite the ubiquity of sparse codes in the brain, the role of timing in the relatively few spikes in sparse sensory codes is

Contacts: Mark Stopfer, 35 Lincoln Drive, Room 3E-623, MSC 3715, Bethesda, MD 20892, USA, Phone: (301) 451-4534, stopferm@mail.nih.gov. Nitin Gupta, Department of Biological Sciences and Bioengineering, Indian Institute of Technology, Kanpur, 208016, India, guptan@iitk.ac.in.
[*]**Current Address:** Department of Biological Sciences and Bioengineering, Indian Institute of Technology, Kanpur, 208016, India. guptan@iitk.ac.in

Author Contributions
N.G. and M.S. designed the experiments; N.G. performed the experiments and analyzed data; N.G. and M.S. wrote the paper.

unknown. Here we sought to answer this fundamental question: whether the timing of sparsely-firing neurons conveys sensory information to their follower neurons.

A remarkable example of sparse sensory coding is found in the mushroom body, an area of the insect brain investigated for roles in olfactory coding and associative learning[8–11]. Kenyon cells (KCs), the intrinsic neurons of the mushroom body, receive olfactory input directly from projection neurons (PNs) of the antennal lobe (analogous to mitral cells of the olfactory bulb) (Fig. 1a). While any given PN shows abundant spontaneous activity and responds to many odors with dense patterns of spikes, KCs are nearly silent at rest and respond selectively to odors, with very few spikes[12]. These highly sparse responses are thought to be advantageous[1] for distinguishing odors and learning associations[13]. Although these rare spikes may occur with different timing relative to the odor presentation in different KCs[14], it is unknown whether this timing is used downstream[13]; information in sparse sensory responses is thought to be coded by the identities of the responding neurons. In motor areas the timing of sparse firing may be used to generate timed motor sequences[15], but in sensory areas sparse coding is viewed as an outcome of, rather than as a substrate for, temporal processing[12, 13]. For example, piriform cortex neurons, which exhibit sparse responses[6] and are morphologically analogous to KCs[16], are thought not to use temporal coding[17], even though their responses are driven by a temporal code in the olfactory bulb.

We tested whether the timing of sparse spikes in KCs carries information to, and affects the responses of, downstream neurons. We performed our experiments in the locust olfactory system, which has been characterized in great detail in terms of anatomy[18, 19], physiology[12, 20] and behavior[21, 22]. Using the types of odors that locusts can discriminate[22], we observed responses of KCs with extracellular recordings, and found that the sparse spikes in KCs occur with odor-specific timing. We then characterized the followers of KCs in the mushroom body using intracellular dye-labeling, mass-fills, and immunostaining. With intracellular recordings, we found that these followers contain information about odor identity in the temporal patterns of their spikes. Finally, using electrical microstimulation of subsets of KCs, we found that the spike patterns in the followers are strongly affected by subtle variations in the absolute or the relative timing of KC spikes. Taken together, our results establish that even the remarkably sparse spiking responses of KCs provide information through odor-specific variations in timing on the order of tens to hundreds of milliseconds, and that these variations determine responses downstream.

Results

Odor-specific timing in KC responses

Extracellular recordings from KCs in awake locusts confirmed very low firing rates (0.05Hz background, 1.21Hz during odor-responses, n=404 cell-odor combinations). Notably, the timing of odor-elicited spikes relative to odor-onset could vary, sometimes by hundreds of milliseconds, with the identity of the odor (Fig. 1b1). Further, different KCs could respond to the same odor with different timing (Fig. 1b2). These results raise the possibility that timing carries sensory information in the sparse spiking of KCs to downstream neurons.

Followers of KCs in the β-lobe of the mushroom body

To understand information transfer downstream from KCs, we first needed to better characterize the projection patterns and odor-elicited responses of follower neurons. KCs project to lobes of the mushroom body where they synapse onto several types of cells, including β-lobe neurons (bLNs)[9, 23–25]. Our intracellular fills revealed several distinct classes of bLNs (Fig. S1, S2). Our analysis focused on the two classes, ‘bLN1’ and ‘bLN2’ (Fig. 1c), identified most frequently in our survey (19% and 60%, respectively, of 83 intracellular fills). Immunostains for GABA were negative for bLN1, but the bLN2 population included both GABA-positive and GABA-negative neurons (Fig. 1d). Our fills of bLN2 showed it sends branches into the calyx of the mushroom body; whether these branches receive input from KCs or provide feedback[9, 25] to the calyx is not clear. It is unlikely that bLN2s receive direct input from PNs because activity in bLN2 can be silenced completely by blocking activity in KCs[20].

Our mass-fill stains identified at least a dozen bLN2s in each hemisphere (Fig. S2). In contrast, several results suggest there is only one bLN1 in each hemisphere. First, mass dye-fills in 5 brain hemispheres showed only one bLN1 per hemisphere, even when large numbers of other bLNs were filled (Fig. S2). Second, with intracellular staining experiments, we never filled in a hemisphere more than one bLN1 despite its large size; by contrast, we routinely found multiple bLN2s, either when we injected dye into multiple cells or on occasions when dye leaked from the electrode (an example is shown in Fig. S4). Third, paired intracellular fills of bLN1 with two different dyes revealed the same neuron (Fig. S3).

bLN2 was previously shown to receive direct input from KCs[24]. Our results suggest bLN1 also receives direct input from KCs: bLN1s extended fine and highly branched, dendrite-like[20] neurites in the β-lobe (see Fig. 1c) and showed reliable, short-latency, excitatory post-synaptic potentials and increased spiking after brief stimulation of KCs (Fig. 2a; also see Fig. 5 below). Consistent with these results, paired recordings showed activating the giant GABAergic neuron (GGN), which inhibits KCs[20, 26], inhibited bLN1 (Fig. 2b). Together, these results established the bLNs as suitable targets for our analysis of KC spike timing.

Temporal patterns of responses in followers of KCs contain odor identity

To understand how the precise timing of KC spikes affects bLN responses, it is useful to understand how bLNs respond to odors. Confirming previous reports from unlabeled neurons in the β-lobe[23, 27], we found both bLN1s and bLN2s fired spontaneously and responded to odors with vigorous bursts of spikes. These dense responses are consistent with the convergence of KCs onto the relatively large dendritic arbors of bLNs (Fig. 1c, S2). In bLNs, the patterns of spikes elicited by odors often endured longer than the odor and contained alternating epochs of excitation and inhibition, each lasting hundreds of milliseconds (Fig. 3a). We found that bLNs of all classes responded to nearly every odor we tested (response probability = 96.9%, n = 262 cell-odor combinations), so the identities of responsive bLNs could not provide enough information to specify the odor. However, different odors could elicit markedly different firing patterns from a given bLN (Fig. 3a; also see Fig. S4); thus, using standard statistical classification methods, we could use these

temporal patterns to classify odor identity (see **Experimental Procedures;** Fig. 3b). Indeed, for both bLN1 and bLN2, within 500 ms of response onset, the single-neuron classification accuracy for a fixed set of 6 odors reached 60–70%, significantly exceeding chance (chance level = 1/6 = 17%; bLN1: $p = 5\times10^{-5}$, n = 6; bLN2: $p = 9\times10^{-5}$, n = 9; two-tailed *t* test); response accuracy continued to improve as longer portions of the response were included in the analysis. Consistent with our response classification results, the odors we used are distinguishable by the animal; hexanol and octanol, which are among the most chemically similar odorants in our test panel, are readily discriminated by behaving locusts[22].

Control analysis using a sham response period of 2 s before the odor presentation yielded performance at chance level regardless of the length of the response analyzed (Fig. 3c). The initial ~500 ms of the response were most informative, but each point in time during the response also carried information about odor identity, as shown by a classification analysis performed on sequential bins made from the response period (Fig. 3d; Experimental Procedures). Instantaneous classification accuracy was significantly above chance even 1 s after odor onset (bLN1: p = 0.035, n = 6; bLN2: p = 0.006, n = 9; two-tailed *t* test). We found that a given odorant could evoke different patterns of spiking in different bLNs of the same class in the same brain (Fig. S4). We also tested (see **Experimental Procedures**) how well odors could be identified given two other characteristics of the response: the mean spike-rate[17] or spike-phase with respect to the simultaneously recorded oscillation cycle[28, 29]. Classification attempts using these features were significantly less successful than classification using temporal patterning (Fig. 3e).

These results show that bLNs contain information about odor identity in temporally structured patterns of spikes. To test whether these response patterns are robust to variations in the number and duration of odor presentations, we measured responses of bLNs to a set of odors presented in 4 different stimulus patterns (Fig. 4a). The responses of bLNs to an odor varied with the presentation pattern of the odor, but retained similarities across the presentation patterns. Thus, a classifier trained on responses evoked by odors presented in one pattern could perform well above chance given responses to other presentation patterns (Fig. 4b), even when the response magnitude was normalized (Fig. 4c).

Temporal patterns in KC responses determine temporal patterns in bLN responses

To determine whether the precise timing of the sparse spikes in KCs carries useful information, it is critical to test whether this timing is actually used by the follower neurons. Our results show bLNs contain information about odor identity in the temporal patterns of their spikes. The precise timing of spikes in KCs could potentially shape the information-rich temporal patterns of spikes in bLNs; if so, this would establish the importance of timing in the sparse responses of KCs. But it is also possible that the fine details of timing of KC spikes are ignored by bLNs as they integrate their input[13]; the odor-evoked temporal patterns in bLNs could instead originate elsewhere, such as with local interactions[27], for example, between GABA-positive and GABA-negative neurons in the β-lobe (Fig. 1d).

To test for causal links between the timings of responses in KCs and bLNs, we manipulated the absolute or the relative timing of spikes in KCs while making intracellular recordings from bLNs (Fig. 5a). To generate sparse[30] and distributed responses in KCs we delivered

low-amplitude current through multiple microwires targeting the KC somata layer in the calyx. Our brief (50, 150 or 300 ms) trains of high-frequency (100 or 200 Hz) electrical stimulation likely elicited in each responding KC only one or a few spikes because KCs show strong spike-frequency adaptation, long-lasting hyperpolarizations following spikes[19], and firing rates that saturate at 10–20 spikes/s in response to current injections[31, 32]; see Fig. S5. Further, bLNs driven by electrically-activated KCs fired at moderate rates matching those evoked by odors (Fig. 5b). Neurons of class bLN2 extend branches into the calyx region of the mushroom body (see Fig. 1c), raising the potential concern that electrical stimulation may have directly activated these cells rather than, as intended, driving them indirectly via the KCs. However, direct activation is unlikely for several reasons. First, we positioned the stimulating electrodes in the KC soma layer, which exclusively contains KCs and is separate from the neuropil region of the calyx[19]. Second, we placed both stimulation anode and cathode in the somata layer to contain the current path within that layer. Third, bLN1s, which do not project to the calyx, responded to electrical stimulation similarly, and as strongly, as bLN2s (Fig. 5c), showing that our results do not depend on direct stimulation of bLNs. These results show our electrical stimulation paradigm evoked activity in KCs, and then in bLNs, well within the spiking range normally evoked by odors.

We first varied the absolute timing of KC stimulation while keeping net stimulation constant by delivering through all wires two different stimulation patterns: 4 epochs of 150-ms stimulation with 100-ms gaps; and 2 epochs of 300-ms stimulation with a 200-ms gap. When KCs were driven this way bLNs responded reliably with firing patterns that could be used to classify the KC stimulation pattern with ~80% accuracy (Fig. 5c,d). We next tested whether bLNs could differentiate a 100-ms epoch of KC stimulation from two 50-ms epochs separated by brief delays ranging from 10 to 200 ms. Indeed, the responses elicited in bLNs by these different patterns could be differentiated with accuracy approaching 100% for delays 100 ms or larger, ~80% for 25 ms, and ~65% for 10 ms (Fig. 5e,f). These results show bLNs are sensitive to changes in KC spike timing on a scale of tens of milliseconds.

Next, we varied the order in which different KCs were stimulated, keeping the absolute stimulation times and net stimulation unchanged. Using a switching circuit directing the same electrical stimulus sequentially to 4 pairs of wires, we activated 4 sets of KCs in different orders, with 50-ms pulses separated by 100-ms delays between sets (Fig. 6a,b1). We found that responses evoked in bLNs depended on the sequence used to stimulate KCs, and could be used to discriminate among 4 stimulation sequences with >95% accuracy (Fig. 6b2). Discrimination performance remained well above chance even when the algorithm was given shorter or longer response durations for classification. The different KC stimulation sequences not only affected the response patterns of bLNs but also their firing rates: classification using the total number of evoked spikes performed less well than classification using patterning, but still better than chance (accuracy = 57% compared to 25% chance, $p = 0.003$ for 500-ms interval; accuracy = 48%, $p = 0.005$ for 1-s interval). We then sought to mimic the smallest realistic change in the relative timing of KCs, which respond to odors with at most one spike per ~50-ms oscillation cycle[12]. We used two sequences of KC stimulation: first, we activated 4 sites sequentially for 50 ms each with no delay between sites; second, we used the same first and fourth site, but interchanged the

order of the second and the third sites (Fig. 6c1). We found even this subtle change could be decoded from bLN response patterns with >80% accuracy (Fig. 6c2); classification accuracy using total number of spikes in a 500-ms period was 66% compared to 50% chance, $p = 0.036$. These results show that minimal variations, on a scale of tens of milliseconds, in the timing of very sparse spikes strongly influence the responses of follower neurons, and thus establish the importance of timing in a sparse sensory code.

Because the experiments using electrical stimulation were performed in the absence of odors (and odor-evoked oscillations), the observed sensitivity of bLNs to KC spike timing did not depend on oscillatory dynamics. The sensitivity of bLNs to precise timing may emerge because different KCs make synapses of different strengths, or at different locations[33], on the dendritic trees of bLNs. For instance, the black stimulation site in Fig. 6b1 and the light blue stimulation site in Fig. 7a appeared to elicit stronger responses than other sites. Also, a close examination of bLN responses suggests activating KCs could evoke inhibition, in addition to excitation, in bLNs. The inhibition evoked by one set of KCs could mask the excitation subsequently evoked by another (Fig. 7a), making bLN responses sensitive to the order in which KCs are activated. One source of this inhibition may be intrinsic to bLNs: directly injecting positive current into a bLN could cause a brief subsequent reduction in its spontaneous firing (Fig. 7b), suggesting a form of fatigue. In some bLNs, however, inhibition driven by the activation of KCs could be observed in the apparent absence of preceding excitation, showing that some inhibition in bLNs arises through circuit interactions (Fig. 7c). The second example in Fig. 7c shows that the inhibition could depend on the identity of stimulated KCs, consistent with the idea that the inhibition in bLNs arises partly through circuit interactions, and not exclusively through mechanisms intrinsic to bLNs.

Discussion

Representations of sensory stimuli can change as they move from one population of neurons in the brain to the next. In deeper layers, stimuli are often encoded by relatively few spikes in selective neurons[1, 13]. Information about sensory stimuli has been thought to be carried by the identities of these sparsely responding neurons [13]. However, our results show that the timing of the sparse KC responses also carries olfactory information, and contributes to the information content of dense codes in follower neurons. Thus, stimulus-specific variations in spike timing provide a useful channel to increase the coding capacity of neurons, while retaining the benefits of sparseness.

The presence of information about odors in the timing of spikes early in the olfactory pathway has been shown in both vertebrates and insects[17, 34–38]. Studies of the insect olfactory system have shown that odors elicit patterns of spikes that vary with the odor in receptor neurons and their followers, the PNs[39, 40]. Our results show that neurons further along in the olfactory pathway, the KCs and the bLNs, also contain information about odors in the timing of their spikes. Recently the neural targets of PNs in the lateral horn were also shown to respond with odor-specific temporal patterns of spikes[41]. Because our results showed that both the firing rates and timing of spikes in bLNs are shaped by the timing of KCs, any mechanism reading the output of bLNs will also be sensitive to the timing of the

sparse responses of KCs. Together, these results suggest temporal coding is used throughout the olfactory system. This view is different from one suggested by a study of the mouse olfactory system[17], which argued that a relative time code in the olfactory bulb is converted into a rate code in piriform cortex neurons (which are analogous to KCs). However, other recent reports suggest the existence of odor-specific timing in this region[42]; to determine whether piriform cortex neurons use temporal codes for odors it may be useful to examine the responses of their follower neurons.

Many factors contribute to the generation of temporal structure in the responses of olfactory neurons early in the olfactory pathway including the physical kinetics of odor delivery and the biochemical chain of events surrounding olfactory transduction[40]. But these factors do not fully explain the temporal patterning observed in bLNs. Indeed, a given odorant could generate nearly identical responses in a given bLN over repeated presentations, but very different response patterns in different bLNs (see responses to 10% hexanol in Fig. 3a; also see Fig. S4). The temporal patterns of response in bLNs, therefore, reflect neuron-specific dynamics, determined by the response patterns of their presynaptic KCs (Fig. 6), possibly with contributions from additional mechanisms within and around the bLNs or lateral connections among KC axons[43]. Our results suggest both intrinsic and network inhibition in bLNs may help to make these neurons sensitive to the timing of KC spikes (Fig. 7). These results also suggest a new functional role for the lateral inhibition observed among bLNs[27].

Although the responses of bLNs clearly contain information about odorants, the precise roles these neurons play in olfactory behaviors remain to be determined. The response patterns in bLNs may be helpful for discriminating odors; these patterns were most informative about odor identity in the first few hundred milliseconds of odor presentation (Fig. 3), consistent with the fast odor discrimination observed in behavioral experiments[44]. The response patterns, however, continued to provide information about odor identity for durations matching or exceeding the duration of the stimulus. This additional information may become useful as the difficulty of the behavioral task increases[45, 46], or when accuracy is more rewarding than speed. It is also possible that the response patterns of bLNs are not needed for discriminating odors per se, but rather for other processes such as encoding memories in the mushroom body, a process that could occur relatively slowly: an insect can learn to associate an odor with a reward, even when the two stimuli are separated by several seconds[47]. If associative olfactory memories involve spike timing-dependent plasticity (STDP) at KC-bLN synapses[27], the odor-specific temporal patterns in KCs and bLNs will determine which subset of the synapses formed by odor-responsive KCs undergo plasticity.

Experimental Procedures

Animals and preparation

All experiments were performed on restrained, unanesthetized locusts, *Schistocerca americana*, raised in our crowded colony (hundreds of animals per cage), with 12-h dark, 12-h light cycle. Two-month old animals (n = 81) of either sex were used in the

experiments. Animals were immobilized and the brains were exposed, desheathed, and superfused with locust saline at room temperature as described previously[41].

Odor stimulation

Odors were delivered as described previously[41]. Briefly, 20 ml of odorant solutions were placed in 60 ml glass bottles at dilutions of 10%, 1% or 0.1% v/v in mineral oil. Odorants used in our study were: grass volatiles hexanol (hex), octanol (oct), hexanal (hxa) and 1-octen-3-ol (o3l); synthetic compounds cyclohexanone (chx) and ethyl isovalerate (eiv); and non-grass plant volatiles geraniol (ger), citral (cit), and methyl jasmonate (mja).

Sharp intracellular recordings

Intracellular recordings were made from bLN dendrites in the β-lobe[24] using sharp glass micropipettes (60–200 MΩ, filled with 0.5 M potassium acetate or an intracellular dye solution). Paired intracellular recordings of bLNs and GGN were obtained by targeting a bLN in the β-lobe and GGN near the pedunculus of the mushroom body with sharp electrodes. The signals were amplified in bridge mode (Axoclamp-2B; Molecular Devices), further amplified with a DC amplifier (BrownLee Precision), and sampled at 15 or 20 kHz (LabView software; USB-6353 DAQ card; National Instruments).

Intracellular staining

The intracellular dye solution consisted of 1% Neurobiotin (Vector Labs) in 0.2 M LiCl, or 5% Lucifer Yellow (Invitrogen) filled at the electrode's tip with 0.2 M LiCl in the shaft. After recording, to identify bLN morphology, dyes were sometimes injected into the neurons iontophoretically using 0.2–2 nA current pulses at 3 Hz for up to 20 minutes. Neurons belonging to bLN1 class could also be readily identified physiologically; compared to other classes of bLNs they exhibited relatively high background firing rates, low input resistance, and few subthreshold excitatory post-synaptic potentials.

Mass fills

Mass fills were used to complement intracellular staining for morphological analysis of bLNs. Neurobiotin or Lucifer Yellow, in the same concentration used for intracellular staining, was loaded in a blunt glass micropipette (5–25 MΩ). The electrode was lowered into the β-lobe, and the dye was released using 10–20 nA current pulses at 3 Hz for up to 20 minutes. During this procedure, the electrode position was adjusted a few times, mostly in the vertical direction (within ~50 μm), to increase the chances of staining multiple neurons. In some cases, effective mass fills were obtained by sequential intracellular staining of several neurons using sharp electrodes as described above.

Histology

After experiments, brains were dissected out, fixed in 4% paraformaldehyde, and prepared for histology as described previously[41]. Imaging was performed using a confocal microscope (Zeiss LSM 510 or LSM 780), with a 10X (0.3 NA) or 20X (0.8 NA) objective. Confocal stacks were analyzed using public domain software ImageJ (NIH). Images showing neuron morphology are maximum intensity projections through confocal stacks,

and were enhanced for clarity by adjusting brightness, contrast and gamma, and by removing noise patches from the brain surface. Images showing GABA immunostains are single sections from the confocal stack, and were minimally enhanced (using only brightness and contrast adjustments, applied uniformly throughout the image).

Immunostaining

Anti-GABA immunostaining was performed on whole locust brains containing dye-filled neurons as described previously[41], using rabbit anti-GABA primary antibody (Sigma, A2052) and Alexa Fluor 488- or 633-conjugated anti-rabbit IgG secondary antibody (Invitrogen, A-11008 or A-21070). Intracellular staining with Lucifer Yellow was enhanced by antibody staining using anti-Lucifer Yellow primary (Invitrogen, A-5750) and Alexa Fluor 488-conjugated secondary (Invitrogen, A-11008).

Multiunit recordings

Extracellular multiunit recordings were made from KCs using custom twisted-wire electrodes[12] containing up to 8 wires. The signals were preamplified, amplified, and filtered using a 16-channel amplifier (A-M Systems). Data were digitally sampled at 20 kHz. KC spike sorting was performed offline using a custom MATLAB program based on the Spike-O-Matic algorithm[48]. Spike sorting was conservative: we analyzed only those clusters that were unambiguously defined and well-separated from one another throughout the experiment.

Local field potential recordings

Local field potential (LFP) was recorded in the calyx of the mushroom body using either a blunt glass capillary electrode (5–15 MΩ, filled with saline) or one of the channels of the extracellular twisted-wire electrodes. The LFP was used to estimate the phases of the spikes of bLNs.

Electrical microstimulation

Because the soma layer dorsal to the mushroom body calyx includes only KC somata[19], we could readily and exclusively target KCs for electrical stimulation. Brief trains of optically isolated current stimulation (IsoStim01-D, NPI Electronic) were delivered at 100 or 200 Hz. We used biphasic stimulation pulses of small amplitude, in either constant current mode (1–4 μA) or constant voltage mode (0.5–5 V, 100–200 kΩ electrode resistance) with pulse-width 1–4 ms. The parameters of stimulation were adjusted for each animal to obtain responses in bLNs resembling those elicited by odors, but were kept unchanged within an experiment. The positive and the negative terminals of the stimulator were connected to 3 or 4 channels each of an 8-channel twisted-wire electrode, splayed among the KC somata (covering 50–60% width of the calyx) to achieve distributed activation of KCs. The timing of stimulation was controlled by LabView (National Instruments) software. Stimuli were presented in randomized orders.

Spatially ordered microstimulation

Spatially ordered stimulation of KCs was achieved by routing isolated stimulation to 4 different sites using 4 Magnecraft W117DIP-25 reed DPST relays (Newark Electronics). To achieve fine control over the selection of stimulation sites, we used two 8-channel twisted-wire electrodes held by separate micromanipulators (the intracellular recording electrode was held by a third micromanipulator). Of the 8 channels in each bundle, 4 were selected (quality assessed by their ability to record LFP signals) and connected to the positive or negative terminals of different relays. The sequence of activation was controlled by LabView (National Instruments) software. Stimuli were presented in randomized orders.

Stimulus-triggered averages

To check whether bLN1 receives direct excitatory input from KCs, we delivered a series (several hundred per cell) of very brief (150–300 μs) pulses of extracellular stimulation to KCs, while monitoring the membrane potential in bLN1 dendrites by sharp-electrode intracellular recording. We then constructed the stimulus-triggered average for each cell to detect any excitatory or inhibitory post-synaptic potentials in bLN1 following stimulation pulses. Note that the observed latency between the stimulus delivery and the onset of the excitatory post-synaptic potential in bLN1 includes the delay in generation of KC spikes after stimulation, the delay in the conduction of spike from KC soma in the calyx to neurites in the β-lobe (estimated[24] to be around ~5.5 ms), and the delay at the synapse.

Data analysis

All analyses were performed using custom programs in MATLAB (MathWorks). All data in the manuscript are reported as mean ± s.e.m. Statistical tests were performed using two-tailed *t* tests or ANOVA. The samples compared were of equal sizes, and did not show significant deviation from normality (Anderson-Darling test). Sample sizes were 6–9 for all tests; significant p-values were well below 0.05. Phases of spikes with respect to the LFP were estimated by measuring their positions relative to the previous (0 radian) and the next (2π radians) peak in the simultaneously recorded LFP (noncausal band-pass filtered, 15–30 Hz).

Determination of odor-responses

Responsiveness of a neuron to an odor was determined by an automated algorithm, using previously published criteria for response amplitude and reliability[12]. To satisfy the amplitude criterion, the neuron's instantaneous firing rate (peri-stimulus timing histogram computed using 20-ms bins and smoothed with a Gaussian of 60-ms s.d.) during the response period (2 s from odor onset) had to exceed more than 3.5 s.d. of the baseline firing rate (computed for 2 s before odor presentation). To satisfy the reliability criterion, the neuron had to fire at least one spike during the 2-s response window in more than half of the trials. We validated these criteria by estimating the false positive rate: the fraction of cell-odor combinations that qualified as responsive in a sham response period (2 s before odor presentation) was small (2.3%).

Classification analyses

Classification analyses were performed on individual neurons using a standard template-matching algorithm[41] with 2-fold non-stratified cross-validation. Briefly, responses of bLNs were represented by vectors of spikes binned in 100 ms windows (other bin sizes gave similar results; Fig. 6b2) when using temporal patterns, or by single bins containing the average spike-rate or average spike-phase (with respect to the simultaneously recorded LFP) when using these other features for classification (Fig. 3e). The classifier first generated a template for each stimulus by calculating the centroid of the vectors from training trials (50% of all trials), and then classified the remaining (test) trials based on Euclidean distance to provide an accuracy estimate. Chance level is given by 1/x, where x is the number of odors or stimulation sequences to be classified (different for different figures). For 0 vector length, accuracy was, by definition, at chance. Control analyses using a sham response period (2 s before stimulus presentation) showed classification accuracy near chance level (Fig. 3c). To test information content in different parts of the response, we used a variant of the above algorithm: the Euclidean distance was computed using the values in the individual bin at each time point (Fig. 3d).

Supplementary Material

Refer to Web version on PubMed Central for supplementary material.

Acknowledgments

We thank members of the Stopfer lab and Maxim Bazhenov for helpful discussions, George Dold and Bruce Pritchard for help with the current stimulation setup, and Kui Sun for her excellent animal care. Microscopy was performed at the Microscopy & Imaging Core (NICHD) with the kind assistance of Vincent Schram. This work was supported by an intramural grant from NIH-NICHD to M.S.

References

1. Olshausen B, Field DJ. Sparse coding of sensory inputs. Curr Opin Neurobiol. 2004; 14:481–7. [PubMed: 15321069]
2. Vinje WE, Gallant JL. Sparse coding and decorrelation in primary visual cortex during natural vision. Science. 2000; 287:1273–6. [PubMed: 10678835]
3. Tolhurst DJ, Smyth D, Thompson ID. The sparseness of neuronal responses in ferret primary visual cortex. J Neurosci. 2009; 29:2355–70. [PubMed: 19244512]
4. DeWeese MR, Wehr M, Zador AM. Binary spiking in auditory cortex. J Neurosci. 2003; 23:7940–9. [PubMed: 12944525]
5. Jadhav SP, Wolfe J, Feldman DE. Sparse temporal coding of elementary tactile features during active whisker sensation. Nat Neurosci. 2009; 12:792–800. [PubMed: 19430473]
6. Poo C, Isaacson JS. Odor representations in olfactory cortex: “sparse” coding, global inhibition, and oscillations. Neuron. 2009; 62:850–61. [PubMed: 19555653]
7. DiLorenzo, PM.; Victor, JD. Spike timing: mechanisms and function. DiLorenzo, PM.; Victor, JD., editors. CRC Press; 2013.
8. Keene AC, Waddell S. Drosophila olfactory memory: single genes to complex neural circuits. Nat Rev Neurosci. 2007; 8:341–54. [PubMed: 17453015]
9. Mobbs PG. The Brain of the Honeybee Apis Mellifera. I The Connections and Spatial Organization of the Mushroom Bodies. Philos Trans R Soc B Biol Sci. 1982; 298:309–354.
10. Strube-Bloss MF, Nawrot MP, Menzel R. Mushroom body output neurons encode odor-reward associations. J Neurosci. 2011; 31:3129–3140. [PubMed: 21414933]

11. Perisse E, Burke C, Huetteroth W, Waddell S. Shocking revelations and saccharin sweetness in the study of Drosophila olfactory memory. Curr Biol. 2013; 23:R752–63. [PubMed: 24028959]
12. Perez-Orive J, Mazor O, Turner GC, Cassenaer S, Wilson RI, Laurent G. Oscillations and sparsening of odor representations in the mushroom body. Science. 2002; 297:359–65. [PubMed: 12130775]
13. Laurent G. Olfactory network dynamics and the coding of multidimensional signals. Nat Rev Neurosci. 2002; 3:884–95. [PubMed: 12415296]
14. Stopfer M, Jayaraman V, Laurent G. Intensity versus identity coding in an olfactory system. Neuron. 2003; 39:991–1004. [PubMed: 12971898]
15. Hahnloser RHR, Kozhevnikov A, Fee MS. An ultra-sparse code underlies the generation of neural sequences in a songbird. Nature. 2002; 419:65–70. [PubMed: 12214232]
16. Sosulski DL, Bloom ML, Cutforth T, Axel R, Datta SR. Distinct representations of olfactory information in different cortical centres. Nature. 2011; 472:213–6. [PubMed: 21451525]
17. Haddad R, Lanjuin A, Madisen L, Zeng H, Murthy VN, Uchida N. Olfactory cortical neurons read out a relative time code in the olfactory bulb. Nat Neurosci. 2013; 16:949–57. [PubMed: 23685720]
18. Kurylas AE, Rohlfing T, Krofczik S, Jenett A, Homberg U. Standardized atlas of the brain of the desert locust, Schistocerca gregaria. Cell Tissue Res. 2008; 333:125–45. [PubMed: 18504618]
19. Laurent G, Naraghi M. Odorant-induced oscillations in the mushroom bodies of the locust. J Neurosci. 1994; 14:2993–3004. [PubMed: 8182454]
20. Papadopoulou M, Cassenaer S, Nowotny T, Laurent G. Normalization for sparse encoding of odors by a wide-field interneuron. Science. 2011; 332:721–5. [PubMed: 21551062]
21. Simoes P, Ott SR, Niven JE. Associative olfactory learning in the desert locust, Schistocerca gregaria. J Exp Biol. 2011; 214:2495–503. [PubMed: 21753041]
22. Saha D, Leong K, Li C, Peterson S, Siegel G, Raman B. A spatiotemporal coding mechanism for background-invariant odor recognition. Nat Neurosci. 2013; 16:1830–9. [PubMed: 24185426]
23. MacLeod K, Backer A, Laurent G. Who reads temporal information contained across synchronized and oscillatory spike trains? Nature. 1998; 395:693–8. [PubMed: 9790189]
24. Cassenaer S, Laurent G. Hebbian STDP in mushroom bodies facilitates the synchronous flow of olfactory information in locusts. Nature. 2007; 448:709–13. [PubMed: 17581587]
25. Li Y, Strausfeld NJ. Multimodal efferent and recurrent neurons in the medial lobes of cockroach mushroom bodies. J Comp Neurol. 1999; 409:647–63. [PubMed: 10376745]
26. Lin AC, Bygrave AM, de Calignon A, Lee T, Miesenböck G. Sparse, decorrelated odor coding in the mushroom body enhances learned odor discrimination. Nat Neurosci. 2014; 17:559–568. [PubMed: 24561998]
27. Cassenaer S, Laurent G. Conditional modulation of spike-timing-dependent plasticity for olfactory learning. Nature. 2012; 482:47–52. [PubMed: 22278062]
28. Hopfield JJ. Pattern recognition computation using action potential timing for stimulus representation. Nature. 1995; 376:33–6. [PubMed: 7596429]
29. Rojas-Líbano D, Kay LM. Olfactory system gamma oscillations: the physiological dissection of a cognitive neural system. Cogn Neurodyn. 2008; 2:179–94. [PubMed: 19003484]
30. Histed MH, Bonin V, Reid RC. Direct activation of sparse, distributed populations of cortical neurons by electrical microstimulation. Neuron. 2009; 63:508–22. [PubMed: 19709632]
31. Demmer H, Kloppenburg P. Intrinsic membrane properties and inhibitory synaptic input of kenyon cells as mechanisms for sparse coding? J Neurophysiol. 2009; 102:1538–50. [PubMed: 19553491]
32. Tabuchi M, Inoue S, Kanzaki R, Nakatani K. Whole-cell recording from Kenyon cells in silkmoths. Neurosci Lett. 2012; 528:61–6. [PubMed: 22981347]
33. Branco T, Clark B, Häusser M. Dendritic discrimination of temporal input sequences in cortical neurons. Science. 2010; 329:1671–5. [PubMed: 20705816]
34. Schoppa NE. Spike timing improves olfactory capabilities in mammals. Neuron. 2010; 68:329–31. [PubMed: 21040837]
35. Smear M, Shusterman R, O'Connor R, Bozza T, Rinberg D. Perception of sniff phase in mouse olfaction. Nature. 2011; 479:397–400. [PubMed: 21993623]

36. Bathellier, B.; Gschwend, O.; Carleton, A. Temporal Coding in Olfaction. In: Menini, A., editor. The Neurobiology of Olfaction. CRC Press; Boca Raton (FL): 2010. p. 329-351.
37. Kay, LM. Advances in Cognitive Neurodynamics (III). Springer; 2013. Timing at Multiple Scales in Olfactory Perception; p. 17-22.
38. Balu R, Larimer P, Strowbridge BW. Phasic stimuli evoke precisely timed spikes in intermittently discharging mitral cells. J Neurophysiol. 2004; 92:743–53. [PubMed: 15277594]
39. Raman B, Joseph J, Tang J, Stopfer M. Temporally diverse firing patterns in olfactory receptor neurons underlie spatiotemporal neural codes for odors. J Neurosci. 2010; 30:1994–2006. [PubMed: 20147528]
40. Su CY, Martelli C, Emonet T, Carlson JR. Temporal coding of odor mixtures in an olfactory receptor neuron. Proc Natl Acad Sci U S A. 2011; 108:5075–80. [PubMed: 21383179]
41. Gupta N, Stopfer M. Functional analysis of a higher olfactory center, the lateral horn. J Neurosci. 2012; 32:8138–48. [PubMed: 22699895]
42. Carlson KS, Xia CZ, Wesson DW. Encoding and representation of intranasal CO2 in the mouse olfactory cortex. J Neurosci. 2013; 33:13873–81. [PubMed: 23966706]
43. Nowotny T, Rabinovich MI, Huerta R, Abarbanel HDI. Decoding temporal information through slow lateral excitation in the olfactory system of insects. J Comput Neurosci. 2003; 15:271–81. [PubMed: 14512751]
44. Vickers N, Baker T. Latencies of behavioral response to interception of filaments of sex pheromone and clean air influence flight track shape in Heliothis virescens (F.) males. J Comp Physiol A. 1996; 178:831–847.
45. Wright GA, Carlton M, Smith BH. A honeybee's ability to learn, recognize, and discriminate odors depends upon odor sampling time and concentration. Behav Neurosci. 2009; 123:36–43. [PubMed: 19170428]
46. Rinberg D, Koulakov A, Gelperin A. Speed-accuracy tradeoff in olfaction. Neuron. 2006; 51:351–8. [PubMed: 16880129]
47. Ito I, Ong RCY, Raman B, Stopfer M. Sparse odor representation and olfactory learning. Nat Neurosci. 2008; 11:1177–84. [PubMed: 18794840]
48. Pouzat C, Mazor O, Laurent G. Using noise signature to optimize spike-sorting and to assess neuronal classification quality. J Neurosci Methods. 2002; 122:43–57. [PubMed: 12535763]

Highlights

1. The timing of spikes in a sparse neural code conveys sensory information
2. Sparse olfactory responses in Kenyon cells occur with odor-specific timing
3. Followers of Kenyon cells use temporal patterns of spikes to represent odors
4. Timing of spikes in Kenyon cells shapes the temporal patterns of these followers

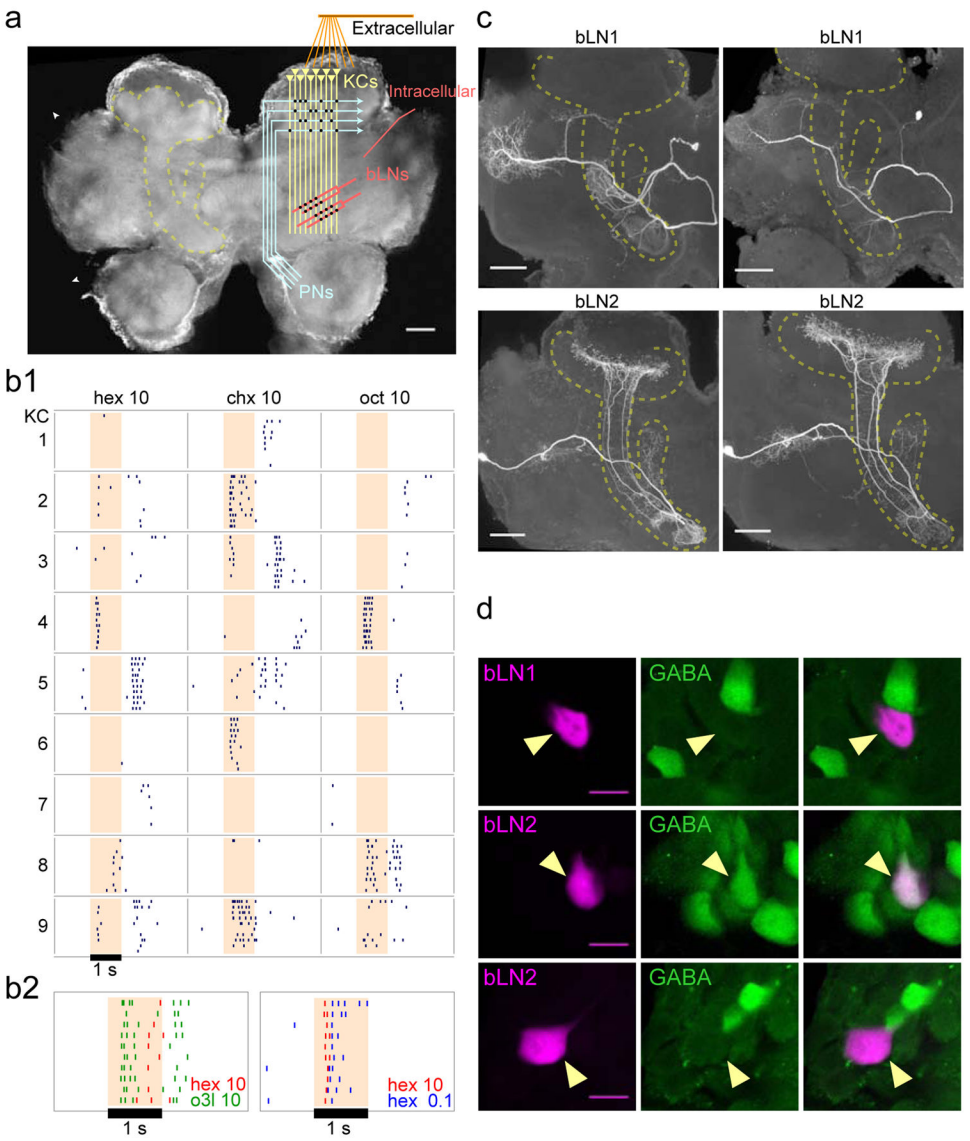

Figure 1.

Responses and followers of KCs. **(a)** Schematic of the locust olfactory system and recording positions. KCs receive input from projection neurons (PNs) in the calyx and send output to α- and β-lobes of the mushroom body (MB). KC somata are located superficially to the calyx. **(b1)** Extracellular recordings from several KCs show sparse responses with odor-specific timing. **(b2)** Superimposed rasterized spiking responses of a single KC to two odors (left) and of another KC to two concentrations of the same odor (right) show odor-specific spike timing; hex, chx, oct, and o3l indicate odors, while 10 and 0.1 indicate percent dilutions (see **Experimental Procedures** for a description of odors). **(c)** Intracellular stains show stereotyped morphologies of bLN1 and bLN2 neurons in different animals (dashed outline: mushroom body). **(d)** Immunostains for GABA show bLN1s are GABA-negative (top, observed >5 times), while bLN2s can be GABA-positive (middle, observed 4 times) or GABA-negative (bottom, observed >5 times); observation counts include cells identified

from intracellular recordings and mass-fills. Scale bars: 100 μm (a and c), 15 μm (d). See also Figs. S1, S2 and S3.

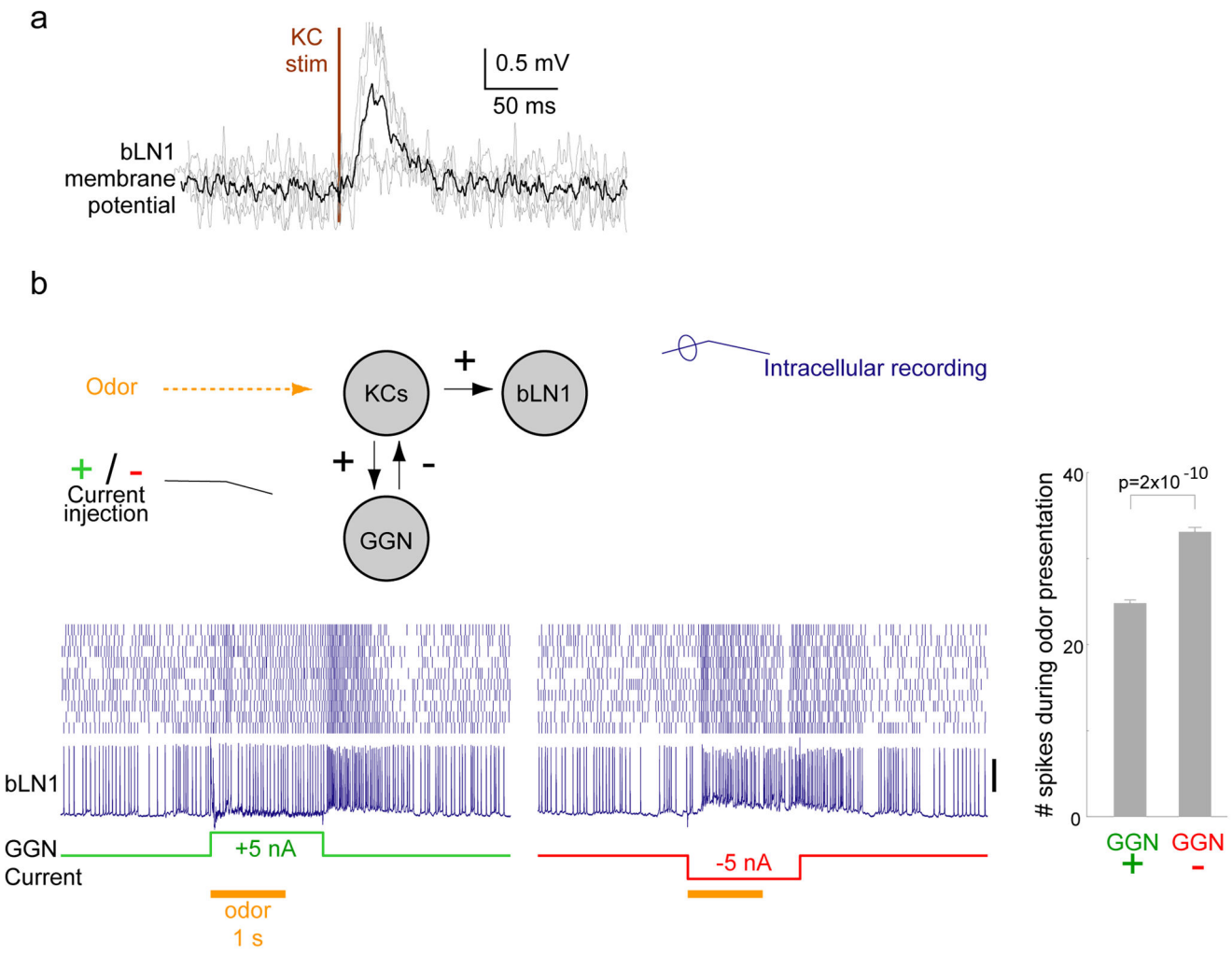

Figure 2.

bLN1 receives direct input from KCs. **(a)** Average membrane potential of individual bLN1 neurons (n = 5, grey) triggered on KC stimulation pulse shows short-latency excitatory input. Black, average of all neurons. **(b)** GGN inhibits bLN1 activity. Using paired intracellular recordings, we injected positive or negative current in GGN while monitoring responses to odor in bLN1. The morphology of bLN1 was confirmed with intracellular staining. Compared to the injection of negative current, injection of positive current in GGN significantly reduced the number of spikes in bLN1 during 1 second of odor presentation; n=10 trials, $p=2\times10^{-10}$, two-tailed *t*-test. The same result was found in another animal (not shown). Scale bar: 20 mV. Error bars show s.e.m.

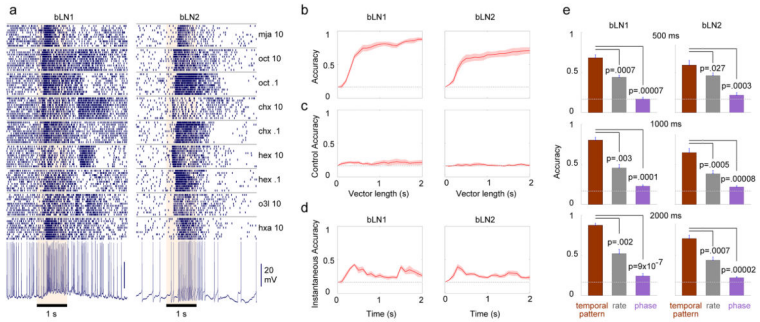

Figure 3.

Response patterns in bLNs contain information about odor identity. **(a)** Dense, temporally patterned, and odor-specific responses of representative bLN1 and bLN2 neurons to 0.1% or 10% concentrations of various odors. Note reproducible patterns across 10 trials with each odor. **(b)** Classification accuracy of many bLNs to a set of 6 odors (0.1% and 10% concentrations of hex, chx and oct) exceeded chance (dashed line: 1/6); n = 6 bLN1s, 9 bLN2s. Solid line with shading: mean (across bLNs) with s.e.m. **(c)** Classification accuracy using bLN activity 2 s before odor delivery is at chance level. This control analysis shows that the above-chance performance observed in panel **b** depends on odor-evoked response patterns, and is not due to differences in background firing. **(d)** A modified classification analysis using short instantaneous segments of responses (see **Experimental Procedures**) shows performance above chance throughout the 2 s period. (**e**). Although bLN spikes were phase-locked to 20 Hz LFP oscillations (for both bLN1 and bLN2), the average phase or the average firing rate of spikes performed poorly, compared to the temporal patterns of spikes, on classifying odor identity (bLN1: n=6; bLN2: n=9); error bars: s.e.m. The same result was obtained whether we analyzed responses in intervals of duration 500 ms, 1000 ms or 2000 ms after the onset of odor. See also Fig. S4.

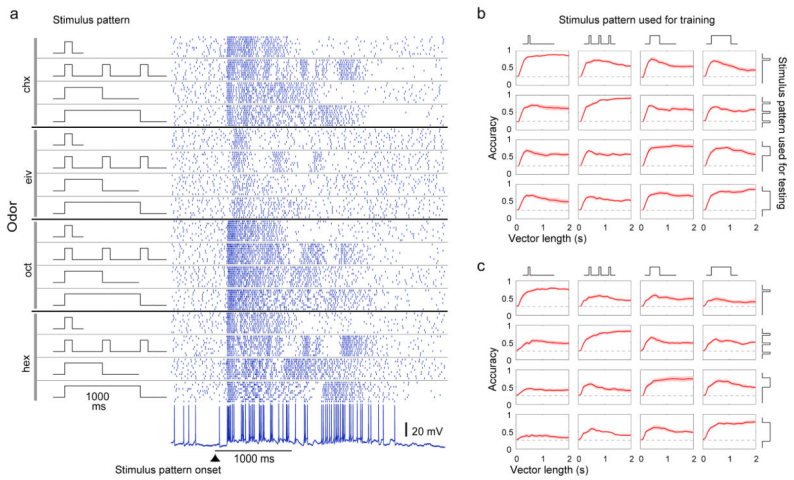

Figure 4.

Odor identity can be extracted from bLN responses even when odor stimulus pattern varies. **(a)** Rasterized spiking responses of a bLN to 4 odors, each presented in 4 different patterns (100 ms, 3×100 ms, 500 ms, and 1000 ms). **(b)** Classification accuracy (n = 11 bLNs) exceeded chance (dashed line = 0.25) even when the classifier was trained on responses to odors presented in one pattern and was tested on responses to the same odor set presented in another pattern. **(c)** Odor identity can be extracted from normalized bLN responses. The magnitude in each response vector (for each trial) was normalized by the total number of spikes occurring 2 s following the onset of odor. The classification accuracy, although less than that observed without normalization of response vectors in panel **b**, exceeds chance (0.25) in all cases. Shading shows s.e.m.

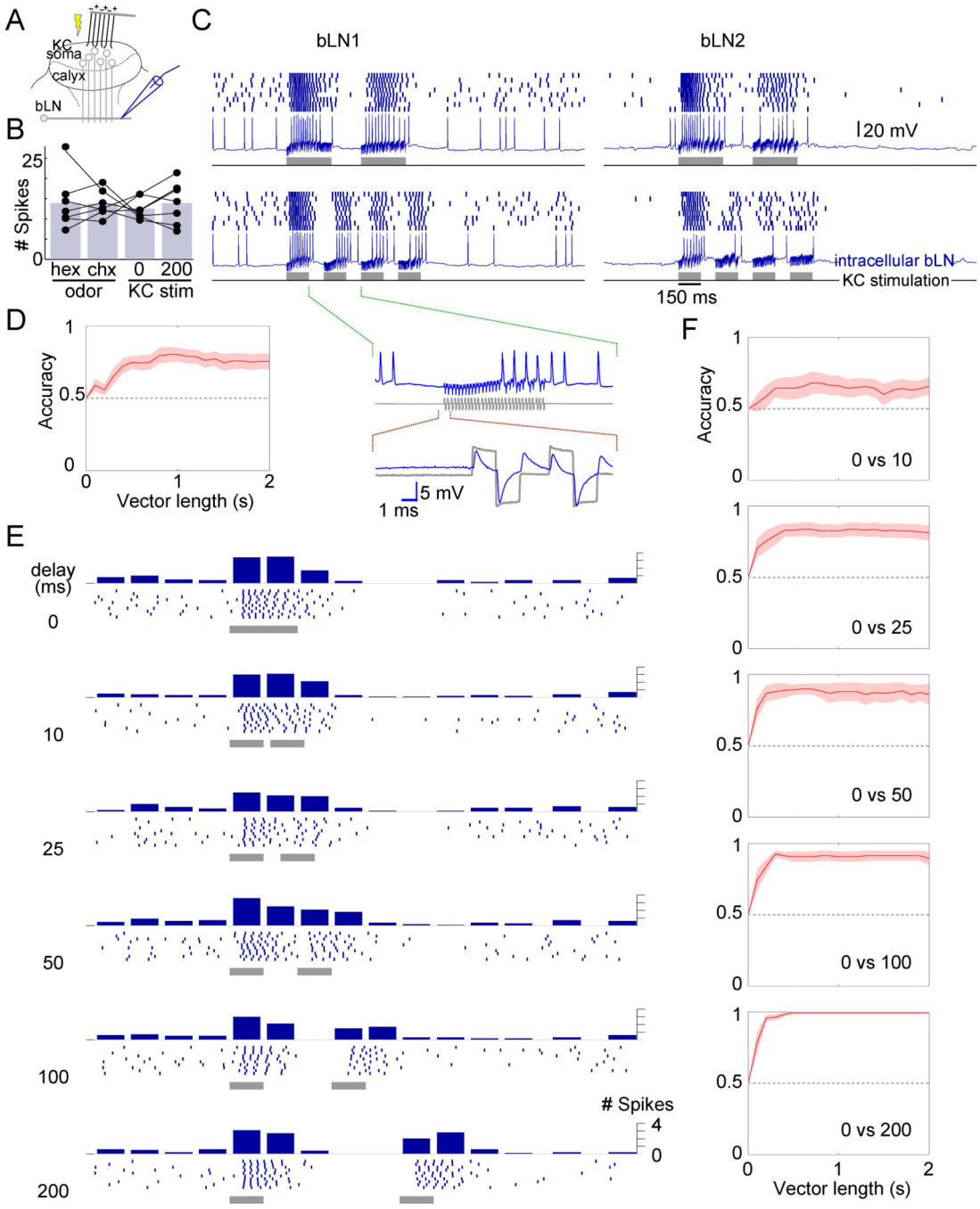

Figure 5.

bLNs are sensitive to changes in the absolute timing of KC activation. **(a)** Experiment setup. **(b)** KC stimulation (a pair of 50-ms pulses separated by 0 or 200 ms delay, see panel **e**) evoked similar numbers of spikes in bLNs (counted in 500 ms from stimulus onset) as did 100-ms pulses of odor (chx or hex) in the same bLNs (n = 7, $F(3,24) = 0.14$, $p = 0.93$, one-way ANOVA); bars show means. **(c)** Responses of representative bLN1 and bLN2 neurons to different temporal patterns of KC stimulation (600 ms total stimulation in both patterns). Inset: detailed view of the intracellular trace (blue) and the simultaneously recorded trace of

the injected current (grey); note the artifacts caused by crosstalk between the stimulator and the recording instrument. These artifacts do not reflect direct activation of bLNs: the artifacts were precisely time-locked with the stimulus trains with virtually no lag (<0.1 ms) but appeared unrelated to spiking; both bLN1 and bLN2 showed similar artifacts even though only bLN2 has branches in the calyx. **(d)** A classifier can differentiate between the two response patterns in panel **c** with high accuracy (chance level = 0.5). Results obtained for different bLN classes were similar and were pooled (n = 15 bLNs). **(e)** Responses of a bLN to pairs of 50-ms pulses separated by different delays. Peri-stimulus time histogram of spikes (binned every 50 ms) is shown above rasters. **(f)** Accuracy of classification between 0-ms delay condition and other delay conditions (n = 8 bLNs). Shading shows s.e.m. See also Fig. S5.

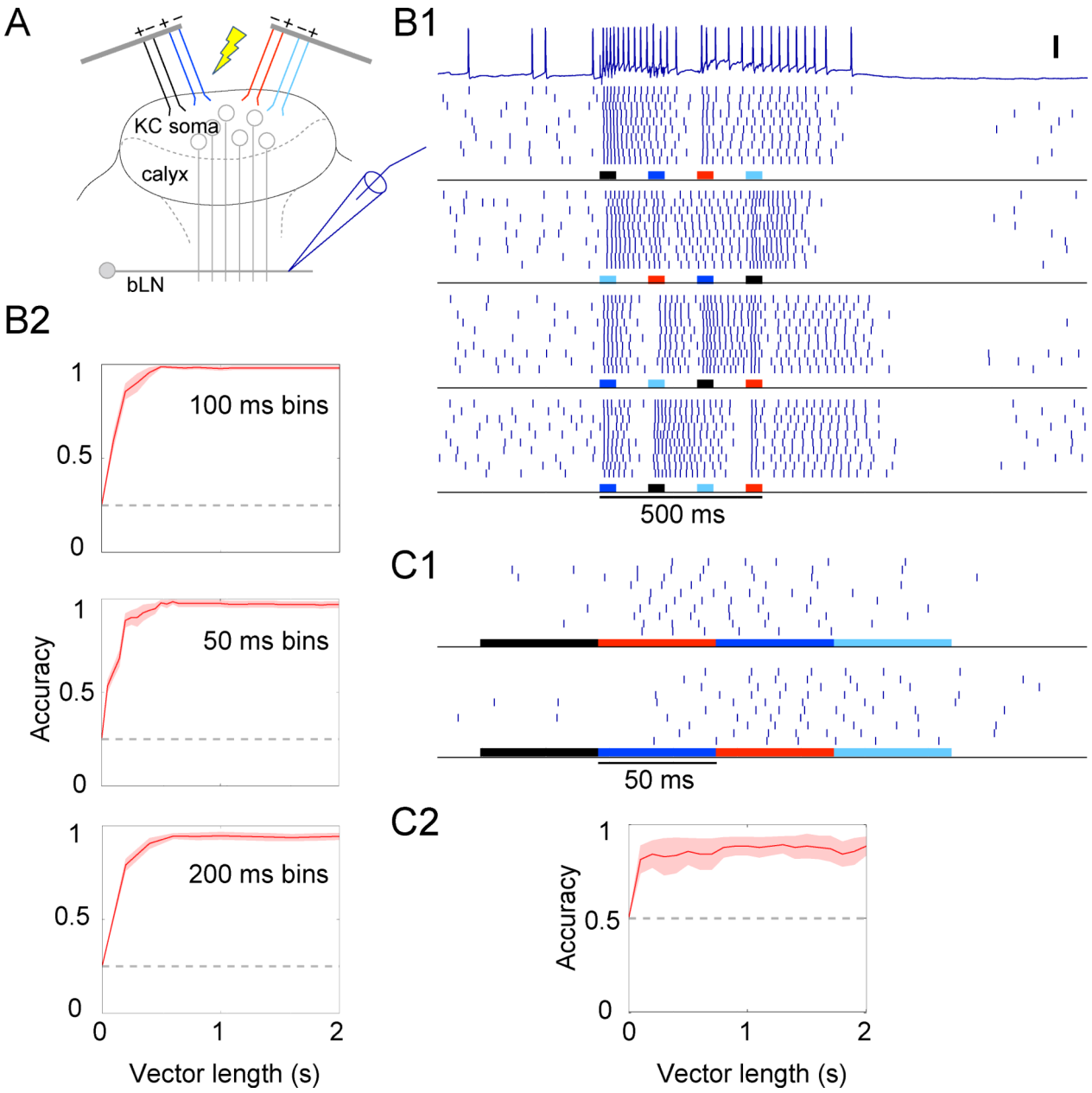

Figure 6.

bLNs are sensitive to the order of KC activation. **(a)** Experiment setup. **(b1)** Responses of a representative bLN to 4 different sequences of KC stimulation. Vertical scale bar: 20 mV. **(b2)** bLN responses can be used to accurately classify the 4 stimulation sequences in panel **b1** (top, n = 8 bLNs, chance level = 0.25); similar results are obtained when the bin size used in the classification analysis is changed from 100 ms to 50 ms or 200 ms. **(c1)** Response of a bLN to two minimally different sequences; note expanded timebase. **(c2)** bLN responses can be used to classify the two stimulation sequences in panel **c1** (bottom, n = 7 bLNs, chance level = 0.5). Shading shows s.e.m.

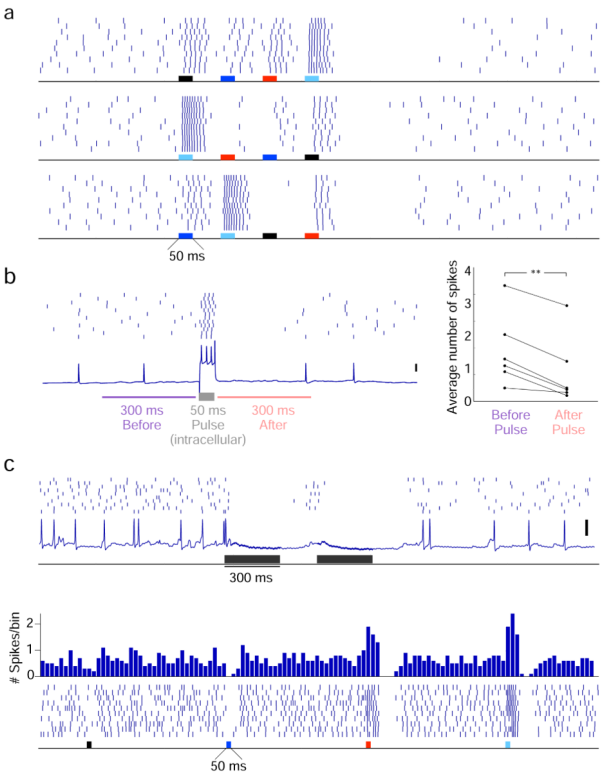

Figure 7.

Inhibition influences bLN response patterns. **(a)** In this representative example, the inhibition caused by stimulation of one set of KCs (light blue electrode) could diminish the excitatory responses normally evoked by other sets of KCs stimulated subsequently; compare responses to the red electrode in the middle panel and the black electrode in the bottom panel with corresponding responses in the top panel. This masking phenomenon was clearly evident in 5 cells. **(b)** Brief, intracellular current pulse injections in bLNs can briefly inhibit subsequent spiking; **p = 0.002, n = 6 bLNs, two-tailed paired *t* test. **(c)** Top, a bLN showing inhibition in absence of excitation following stimulation of KCs. Bottom, a bLN in which stimulation of one set of KCs (dark blue electrode) evoked inhibition (in absence of preceding excitation), while stimulation of other sets of KCs (red and light blue electrodes) evoked both excitation and inhibition. Peri-stimulus time histogram of spikes (binned every 50 ms) is shown on top; inhibition in absence of excitation was observed in 4 cells. Vertical scale bars: 20 mV.